ELSEVIER

Journal of Chromatography B, 770 (2002) 35–43

JOURNAL OF CHROMATOGRAPHY B

www.elsevier.com/locate/chromb

Effect of experimental conditions on strong biocomplimentary pairing in high-performance monolithic disk affinity chromatography

Natalia D. Ostryanina, Olga V. Il'ina, Tatiana B. Tennikova*

Russian Academy of Sciences, Institute of Macromolecular Compounds, 199 004 St. Petersburg, Russia

Abstract

The effect of flow-rate on quantitatively determined binding parameters for several biocomplementary pairs in affinity mode high-performance monolithic disk affinity chromatography (HPMDAC) has been investigated using frontal analysis approach. Affinity interactions were evaluated from linearized adsorption isotherms and dynamic dissociation constants of the complexes $K_{diss.}$ and the theoretical adsorption capacities Q_{max} were calculated. HPMDAC isolation of a typical protein trypsin from both buffered solution and artificial mixture as well as biospecific extraction of antibodies against bovine serum albumin and recombinant protein G from such complex mixtures as blood serum and cellular lysate were examined. Immobilized counterparts soybean trypsin inhibitor, bovine serum albumin, and human immunoglobulin G were used in chromatographic experiments. The maximum adsorption capacities obtained at different flow-rates were compared with those determined at static conditions. The dependence of quantitative parameters on the surface density of immobilized ligands has also been explored. Finally, a series of experiments was carried out to evaluate the dependence of dynamic affinity binding on temperature for two complementary pairs.

Keywords: Biocomplenentary pairing; Monolithic disks

1. Introduction

The polymeric monoliths synthesized in a shape of flat macroporous disks with optimized macroporous inner structure (CIM® Disks, BIA Separations d. o. o., Ljubljana, Slovenia) [1–4] are promising stationary phases for a variety of dynamic processes based on interphase mass transport such as high-performance monolithic disk chromatography (HPMDC) [5–7]. Since such stationary phases contain no particles but only a net of flow-through pores (channels), the mass transfer restrictions typical of porous beads are not observed and extremely rapid processes requiring only seconds could be realized. It is worth noting that the most impressive applications of HPMDC were demonstrated in the area of affinity processes based on specific recognition of natural biological complements [8–12].

In conventional columns affinity chromatography, gel-type or rigid porous particles are used as a stationary phase [13,14]. It is becoming obvious that discrete porous particles, even those having partial flow-through (perfusion) inner structure [15–19], suffer from the serious limitations of slow mass transfer of molecules of any size including both small and very large ones such as proteins that employs diffusion to reach the space within pores. As a result, this slow process represents a time

*Corresponding author.

1570-0232/02/$ – see front matter
PII: S1570-0232(01)00597-9

bottleneck of the whole separation process that involves biocomplementary pairing between immobilized and dissolved complements. Thus, the throughput (productivity) of such an affinity chromatography is significantly dropped. An increase in flow-rate leads to a dramatic deterioration of the separation in these systems.

In contrast, monolithic separation media with the immobilized ligand located on the open surface of the flow-through channels is readily accessible for its specific counterpart present in the flowing mobile phase. These advantageous hydrodynamic properties of monolithic sorbents result from their specifically designed morphology enable observation of the real-time kinetics of formation of bioaffinity pairs upon dynamic conditions. In other words, the mass transfer enhanced by convection allows considering the biospecific reaction as the only time limiting process [7,8].

It has been demonstrated that the flow-rate does not exert any effect on the protein binding capacity in ion-exchange and reversed-phase separations using monolithic disks as a stationary phase [5,20–22]. However, similar experiments have never been carried out in affinity mode of HPMDC despite the indications of positive effects [11]. Considering the ''membrane-like'' format of these supports, the results concerning membrane affinity adsorbers such as those in Refs. [23–28] should be carefully scrutinized. The major issue common for all methods employing very short length of separation layers is *residence time* of a solute in this layer and a ratio of this parameter and the *time required for the soluble counterpart to reach the immobilized ligand*. This effect was clearly demonstrated for IE HPMDC [29].

Besides the effect of the flow-rate on efficiency of affinity interactions, the role of surface coverage density of immobilized specific ligands and temperature are also important variables useful in optimization of high throughput affinity processes.

2. Experimental

2.1. Materials

Monolithic disks 12 mm in diameter and 3 mm thick (CIM® Epoxy Disks) were provided by BIA Separations d. o. o., Ljubljana, Slovenia. The mean pore size measured by mercury intrusion porosimetry was equal to 1 μm whereas porosity was determined as 0.7 ml/ml sorbent. These disks were placed in the specifically designed cartridge also produced by BIA Separations and attached to chromatographic equipment.

Bovine serum albumin (BSA), soybean trypsin inhibitor (SBTI), human immunoglobuline G (*h*IgG), and ovalbumin (OVA) were purchased from Sigma–Aldrich (Diesenhofen, Germany). Trypsin (TR) and α-chymotrypsin (CHTR) from bovine pancreas were from Fluka (Buchs, Switzerland). Recombinant Protein G as well as cellular lysates of *Escherichia coli* with genetically expressed Protein G were kindly donated by Professor T.V. Gupalova from the Institute of Experimental Medicine, Russian Academy of Medical Sciences, St. Petersburg, Russia.

Mixture of polyclonal antibodies against synthetic peptide bradykinin covalently conjugated with BSA [10] was produced and fractionated using procedure published elsewhere [10,12].

All buffers used were prepared by dissolving salts of analytical grade in double distilled water and additionally purified by filtration through a 0.45 μm microfilter Milex (Millipore, Austria).

2.2. Instruments

HPMDAC experiments were performed using a LKB (Uppsala, Sweden) system consisting of a peristaltic pump (Varioperpex 2120), an UV-detector (Unicord S 2138), and a plotter (1-Channel Recorder 2210). Alternatively, a high-performance chromatograph Gilson (Villiens le Bell, France) combining two piston pumps 303 and 305 and a 118 UV–VIS detector was also used.

The UV absorbancy of ligands in solutions used for immobilization (proteins) was determined at different wavelength using an UV spectrophotometer SF-26 (LOMO, St. Petersburg, Russia).

Amino acid analysis was carried out using automatic amino acid analyzer (Amino Acid Analyzer T339 M, Mikrotechna, Prague, Czech Republic).

Enzyme-linked immunosorbent assay (ELISA) was carried out in 96-wells polystyrene microplate (Medpolymer, St. Petersburg, Russia). The optical absorbancy of products of the enzymatic reaction

was detected using a multiscan spectrophotometer (Titertek Multiscan® MCC instrument, Helsinki, Finland).

2.3. Methods

2.3.1. Immobilization procedure

The standard procedure [8] was used for the immobilization of SBTI, BSA, *r*Prot G and *h*IgG on epoxy CIM® Disks. The amount of covalently bound ligand was calculated from the change in absorbancy of solution before and after the reaction. Standard Lowry test [30] was used to determine the protein concentrations. In a few cases, the amount of bound ligand was also determined by amino acid analysis of a small part of the polymeric support.

2.3.2. HPMDAC experiments

The affinity HPMDC comprises a combination of adsorption and desorption steps using a stepwise gradient of a mobile phase. A PBS buffer, pH 7.0, was used in the adsorption whereas the desorption was achieved using 0.01 *M* HCl, pH 2.0. An intermediate washing procedure with 2 *M* NaCl was used to release a protein bound the surface through non-specific (ionic) interactions.

Frontal analysis was used to evaluate the parameters of affinity binding. The adsorption characteristics were investigated by passing of the protein solutions with different concentrations through the affinity disk.

To establish the effect of flow-rate on adsorption capacity, four affinity pairs each representing immobilized ligand and soluble counterpart were studied. The first system involved a disk with immobilized BSA and monofunctional anti-BSA antibodies were isolated from blood serum fraction. In all experiments, 10 ml of antibody solution having always a protein concentration of 0.5 mg/ml were loaded. The second pair was immobilized SBTI and soluble TR with concentrations 0.52, 0.29, 0.055, 0.013 and 0.009 mg/ml at mobile phase flow-rates of 0.5, 2.0, 5.0 and 10 ml/min. In the third and fourth set of experiments, the soluble affinity counterpart was included in complex mixtures such as TR dissolved in a model mixture of BSA, OVA and CHTR, or *r*Prot G in *E. coli* cellular lysates. Immobilized SBTI and *h*IgG were used as the strong affinity ligands, respectively.

The quantitative affinity characteristics of all of the pairs such as maximum affinity adsorption capacity (Q_{max}) and dynamic dissociation constants of affinity complex (K_{diss}), were calculated from experimental adsorption isotherms obtained from frontal analysis [24]. The data are average values calculated from linearized forms of the Langmuir equation.

The static adsorption was performed by immersing the SBTI-CIM® affinity disk into 0.52 and 0.1 mg/ml TR solutions. After 20 h of incubation at room temperature, the disk was washed by pumping a PBS buffer and the desorption achieved using 0.01 *M* HCl.

Temperature-dependent experiments were performed in an ice bath (0 °C) and an air thermostat (15–40 °C). All solutions as well as the cartridges with installed SBTI- and *r*Prot G-CIM® disks were thermostated to the desired temperature. The 0.05–0.5 mg/ml solutions of TR and *h*IgG were passed through the disk at a flow-rate of 2 ml/min to determine the adsorption isotherms and to calculate the affinity parameters.

2.3.3. ELISA-test

The concentration of *r*Prot G in crude *E. coli* cellular lysates was determined using an ELISA test developed recently [31].

3. Results and discussion

3.1. Dynamic approaches to the analysis of porous structure of monolithic sorbents used in HPMDAC

It has been repeatedly claimed that the main advantage of monolithic media in separation processes is the specifically designed and well controlled inner porous space [5–7,20,22,29]. Chromatographic approaches to quantitative evaluation of parameters such as porosity and pore size have already been described [29]. The results appear to be in a good agreement with those calculated from other physical measurements. The morphology of the porous polymer layers is assumed to play even more

important role in affinity chromatography than in IE and RP modes of HPMDC.

It is well known that such monolithic materials have ''biporous'' or, more correctly, a multiporous structure combining the flow through channels of roughly 1 μm in size with smaller interconnected pores contributing to the overall surface area. Using hydrodynamic properties of the porous structure of membrane microfilters, mean pore size of macroporous supports can be calculated. The disks used in this study exhibit a low backpressure even at high flow-rates. For example, Fig. 1 shows the backpressure for different types and batches of CIM® disks as a function of volumetric flow-rate of water. The linear plots indicate that the porous space can be approximated as a cluster of flow-through capillaries with a hydrodynamic resistance depending on their mean pore size (Poiseuille–Darcy equation) [26]. In other words, the flow through a macroporous monolith obeys the rules of laminar flow through a straight cylindrical tube of defined radius and length.

Low backpressures of 0.5–1.8 MPa were observed for the disks at flow-rates of 0.5–20 ml/min. A number of CIM® epoxy disks have been examined and very good batch to batch reproducibility observed. Two examples are presented in Fig. 1.

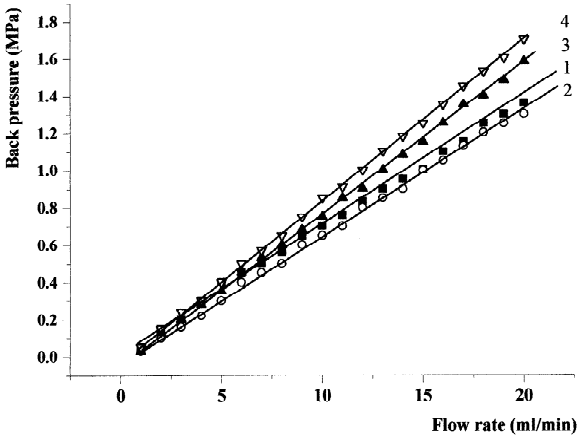

Fig. 1. Effect of backpressure of CIM® disks on flow-rate. Line 1–CIM® epoxy disk, batch 109993; line 2–CIM® epoxy disk, batch 079981; line 3–CIM® epoxy disk from batch 109993 with covalently coupled 0.9 mg CHTR; line 4–CIM® epoxy disk from batch 109993 with covalently coupled 1 mg BSA. *Conditions*: 12×3 mm I.D. CIM® disks installed in a commercial cartridge; mobile phase distilled water; flow-rates 1–20 ml/min.

Similar experiments were carried out using disks with immobilized proteins (BSA and CHTR). It is important that only insignificant changes in back pressure were noted.

Simple calculation using data of Fig. 1 reveals a mean pore size of flow-through channels of 0.3 μm and a total inner surface of 1.8 m^2/ml sorbent. This surface of flow-through pores also represents the surface area participating in the affinity interaction process and allows estimation of density of immobilized affinity ligands.

3.2. Immobilized ligands capacity (surface density)

Variations of experimental conditions recommended recently [8] were used to prepare series of CIM®-BSA and CIM®-SBTI affinity supports with varying ligand density. For example, 8 h long reaction affords 13 n*M* immobilized BSA per 1 m^2 of the pore surface. In contrast, twice as high an amount was found after a reaction time of 16 h. Similar results were achieved in immobilization of SBTI (Table 5).

In addition, using simple equations and geometric approximations, it is also possible to estimate the cross section of protein molecule immobilized on the surface of the flow-through channels and, accordingly, the total surface area covered by immobilized ligands. Accordingly, the surface coverage of flow-through channels was 60–90% out of the maximum ligand density of 1.0 and 1.7 m^2/ml for BSA and SBTI, respectively, was observed.

These data can be considered as an indirect confirmation of maximum immobilization capacity upon conditions used for the covalent coupling. The second conclusion, which can be drawn, is that all flow-through pores or convective channels of our monolithic layers are almost completely covered by affinity ligands that are involved in the separation process.

3.3. Effect of flow-rate on HPMDAC binding capacity (zonal approach)

A simple description of the effect of geometry of flow-through channels on chromatographic separations using thin membrane-like sorbent layer has already been published [23–28]. It has been demon-

strated that the residence time of a solute within the porous space of membrane unit, t_{res}, and the time needed for a solute molecule to traverse the distance between its location within the stream to the pore wall by free diffusion through a superficial stagnant layer of a liquid, t_{film}, control the process. Obviously, the residence time depends on flow-rate of the mobile phase and the thickness of the disk, whereas t_{film} depends on the size of the flow-through pores. For example, t_{res} must sufficiently exceed t_{film} to allow the molecule of a protein to freely diffuse from the stream to the wall of a channel and to bind to the adsorbing functionalities located on the pore wall surface.

HPMDAC experiments revealing the effect of flow-rate on binding parameters have been carried out using defined (fixed) volumes of loaded molecules. Specifically, a pool of polyclonal antibodies against BSA has been chosen as a soluble part of pair and BSA has been immobilized on CIM® epoxy disk as the specific ligand. Binding has been studied using mobile phase flow-rates of 0.5–10.0 ml/min for both adsorption and desorption steps.

According to the literature [6,7,24,25], the residence time of solute within a sorbent layer can be calculated as:

$$t_{res} = L/U \quad (1)$$

and t_{film} as:

$$t_{film} = d_p^2/4D \quad (2)$$

where L is the length of the separation layer, U is the linear flow velocity of a mobile phase, d_p is the pore (channel) diameter, and D is the coefficient of free diffusion of the solute.

Table 1 shows the amounts of anti-BSA antibodies eluted at increasing flow-rates that represent decreasing t_{res} values. Only 2-fold reduction in specific adsorption capacity was observed while decreasing the residence time 20 times (from 24.4 to 1.2 s). It should be noted that even the shortest $t_{res} = 1.2$ s was much longer than the calculated value of t_{film} that equals $2.5\ 10^{-2}$ s. These factors must be taken into consideration in designing a high speed affinity processes using short separation layers as a stationary phase.

Table 1
Effect of flow-rate on the amount of eluted antibodies at fixed volume of loaded sample

Flow rate (ml/min)	Residence time, t_{res} (s)	Amount of eluted antibodies, Q, mg/ml sorbent
0.5	24.4	0.59
2.0	6.1	0.41
5.0	2.5	0.27
10.0	1.2	0.24

Conditions: PBS solution (10 ml) containing 5 mg of polyclonal antibodies was loaded on CIM®-BSA disk at the different flow-rates; intermediate washing step was performed using 2 *M* NaCl and desorption step was carried out with 0.01 *M* HCl (pH 2.0); desorbed fraction of antibodies was collected and analyzed by Lowry test; all experiments were carried out in triplicate with RSD 5–10%.

3.4. Frontal analysis at different flow-rates

To evaluate both the maximum binding capacity, Q_{max}, and the equilibrium constant of dissociation of affinity complex, K_{diss}, which is an important thermodynamic characteristics of the affinity interaction, at different flow-rates, we used the frontal analysis approach. In this case, a loading was continued until the breakthrough has been observed and the absorbancy of the protein solution at the outlet was equal to that at the inlet. At this point, all accessible affinity sites were occupied by specifically adsorbed target molecules.

We used affinity pair soluble trypsin–immobilized soybean trypsin inhibitor (TR-SBTI) as a model in these investigations. The adsorption isotherms resulting from frontal experiments were used for calculation of the discussed parameters. Table 2 shows that the maximum adsorption capacity of CIM®-SBTI disk does not change at different flow-rates since the experimental isotherms obtained at flow-rates of 0.5–10.0 ml/min appear to be very similar. In all these cases, the experimentally determined dissociation constants are close to 0.8 μ*M* confirming that flow-rate has no effect on both maximum capacity and affinity constant.

A more complex system is encountered with a model protein mixture consisting of BSA, OVA, CHTR and TR applied on CIM®-SBTI disk. Table 3 presents results of this series of experiments. Once again, the results do not differ significantly from

Table 2
Dependence of quantity of TR recovered on flow-rate for the different concentrations of loading solution

Flow rate (ml/min)	Loading volume (ml)	C_1 (mg/ml)	Q_1 (mg/ml)	C_2 (mg/ml)	Q_2 (mg/ml)	C_3 (mg/ml)	Q_3 (mg/ml)	C_4 (mg/ml)	Q_4 (mg/ml)	C_5 (mg/ml)	Q_5 (mg/ml)
0.5	3.5	0.520	0.44	0.290	0.41	0.055	0.32	0.013	0.15	0.009	0.12
2.0	5.0	0.520	0.47	0.290	0.41	0.055	0.32	0.013	0.15	0.009	0.12
5.0	9.0	0.520	0.41	0.290	0.38	0.055	0.35	0.013	0.15	0.009	0.15
10.0	15.0	0.520	0.44	0.290	0.38	0.055	0.35	0.013	0.17	0.009	0.12

Conditions: different sample volumes with different concentrations ($C_1, C_2, \ldots C_5$) were pumped through CIM®-SBTI disk at different flow-rate to produce the breakthrough curve; specifically bound (PBS, pH 7.0) TR was desorbed using 0.01 *M* HCl (pH 2.0); desorbed fraction of TR was collected and analyzed by Lowry test ($Q_1, Q_2, \ldots Q_5$ represent obtained amounts of desorbed TR); all experiments were carried out in triplicate with RSD 5–10%.

Table 3
Effect of flow-rate on recovery of TR from model protein mixture

Flow rate (ml/min)	C_1 (mg/ml)	Q_1^* (mg/ml)	Q_1 (mg/ml)	C_2 (mg/ml)	Q_2^* (mg/ml)	Q_2 (mg/ml)
0.5	0.1	0.53	0.38	0.055	0.50	0.35
2.0	0.1	0.53	0.35	0.055	0.47	0.35
5.0	0.1	0.50	0.35	0.055	0.50	0.32
10.0	0.1	0.53	0.35	0.055	0.50	0.35

Conditions: the mixtures containing TR, CHTR, BSA and OVA with different concentrations of TR (C_1, C_2) were pumped through CIM®-SBTI disk at different flow-rates to produce the breakthrough curve; the adsorption and desorption steps were carried out with PBS (pH 7.0) and 0.01 *M* HCl (pH 2.0), respectively; the desorbed amounts of TR Q_1 and Q_2 were obtained with use of intermediate washing step (2 *M* NaCl) whereas Q_1^* and Q_2^* values correspond to the procedure excluding this operation; the amount of eluted protein was determined by Lowry test; all experiments were carried out in triplicate with RSD 5–10%.

those characterizing the simple protein–protein model pair described above. Similarly, affinity CIM®-*h*IgG disk was used for isolation of recombinant Protein G (*r*Prot G) directly from *E. coli* cellular lysate and the results presented in Table 4 are very similar again. It is highly recommended to

Table 4
Effect of flow-rate on *r*Prot G recovery from *E. coli* cellular lysate

Flow rate (ml/min)	Loading volume (ml)	C_1 (mg/ml)	Q_1 (mg/ml)	C_2 (mg/ml)	Q_2 (mg/ml)
0.5	7	0.32	0.68	0.17	0.41
2.0	15	0.32	0.76	0.17	0.41
5.0	35	0.32	0.78	0.17	0.38
10.0	55	0.32	0.74	0.17	0.38

Conditions: cellular lysates previously diluted (1:3) and filtrated with concentration of *r*Prot G equal to C_1 and C_2 were pumped through CIM®-*h*IgG disk at different flow-rates to produce the breakthrough curve; intermediate rinsing procedure with 2 *M* NaCl was carried out and specifically bound *r*Prot G was eluted using 0.01 *M* HCl (pH 2.0) the amount of eluted protein was determined by Lowry test (Q_1 and Q_2 represent obtained amounts of desorbed *r*Prot G); the initial concentration of *r*Prot G was estimated by ELISA method; all experiments were carried out in triplicate with RSD 5–10%.

include an intermediate washing step in the experimental design to avoid the non-specific adsorption of proteins (Table 3).

The results discussed in previous paragraphs indicate that in order to achieve the total saturation of affinity binding sites in HPMADC, the volumes of solute solution that must be passed through the flat separation unit depends on flow-rate. In other words, the higher the flow-rate, the larger the sample volume has to be loaded. In contrast to the other types of HPMDC, the ratio t_{res}/t_{film} is extremely significant in affinity separations and a considerable part of the target molecules just flows through at high flow-rates without being retained. In addition, the kinetics of affinity pairing also appears different compared to ion–ion or hydrophobic interactions. This may result from much lower density of adsorption sites on the pore surface than that available in the typical IE or RP HPMDC modes. As a result, probability of contacts between soluble and immobilized counterparts within a time unit is lower. An increase in the loaded sample volume compensates for the decreased number of effective interactions. This also indicates that the use of extremely high flow-rates in HPMDAC is not recommended. Thus flow-rates of 7–10 ml/min that would be very attractive from the point of time benefit is offset by the lost of valuable biological material. Therefore, flow-rates of 2–5 ml/min are a good compromise allowing to complete the process within a few minutes.

3.5. Binding capacity at static conditions

For a comparison, we also studied the affinity binding capacity in static batch mode using pair TR-SBTI as a model. In contrast to published data concerning membrane affinity adsorbers [23], we found 3-fold lower capacity compared to that observed under the dynamic conditions of frontal analysis. This is likely due to very low diffusivity of protein molecules within a rigid macroporous space in the absence of convective flow [32]. The loading could be probably increased by extending the time of exposition. To confirm this suggestion, the following experimental series has been done. It was shown that the amount of specifically adsorbed TR was increased from 0.06 up to 0.16 mg/ml sorbent at increasing time of exposition from 3 up to 17 h. On the other hand, the approach of using of infinite time of static adsorption includes danger of denaturation of protein complements.

3.6. Effect of ligand density and temperature on affinity binding

The effect of both density (surface concentration) of specific ligands and temperature on affinity binding is demonstrated on pairs TR-SBTI and BSA-antiBSA antibodies (antiBSA Abs). Table 5 shows the results. A 2-fold decrease in ligand concentration does not strongly affect K_{diss} of both affinity complexes whereas the maximum adsorption capacity decreases proportionally. The data also indicate that only 20–25% of immobilized ligands are accessible for a soluble affinity partner to form the specific pair. This result is in a good agreement with those published previously for HPMDAC [8,10]. It should be noted however, that despite the modest adsorption capacity of the monolithic supports, the overall productivity of HPMDAC is really large. For example, up to 10 mg of purest *h*IgG can be isolated from blood plasma in 1 h using CIM®-*r*Prot G disk [31]. Use of both few affinity disks stacked in a cartridge and CIM®-*r*Prot G tube [33] can further increase the throughput of the method.

The effect of temperature in the range 0–40 °C on the affinity binding was studied using pairs TR-SBTI

Table 5
Q_{max} and K_{diss} values for the TR-SBTI and anti-BSA Abs-BSA pairs measured at different density of ligands

Immobilized ligand-soluble counterpart	Ligand density, (nM/m^2)	Q_{max} (nM/m^2)	K_{diss} (μM)
SBTI-TR	63	10.0	0.76
SBTI-TR	30	5.6	0.57
BSA–antiBSA Abs	25	5.6	3.80
BSA–antiBSA Abs	13	2.4	3.00

Conditions: Solutions of TR of 0.01–0.7 mg/ml concentration range and polyclonal antibodies with concentration of 0.05–1 mg/ml were loaded on CIM®-SBTI and BSA disks, respectively, at 2 ml/min flow-rate to produce the breakthrough curves; intermediate washing procedure was performed using 2 *M* NaCl and desorption step was carried out with 0.01 *M* HCl (pH 2.0); desorbed fractions of proteins were analyzed by Lowry test; all experiments were carried out in triplicate with RSD 5–10%.

Table 6
Effect of temperature on affinity pairing

Temperature (°C)	SBTI (immob.)–TR (solub.)		*r*Prot G (immob.)–*h*IgG (solub.)	
	Q_{max} (mg/ml)	K_{diss} (μM)	Q_{max} (mg/ml)	K_{diss} (μM)
0	0.32	0.63	1.29	0.25
15	0.40	0.70	1.85	0.33
20	0.44	0.76	2.00	0.37
40	0.26	0.82	0.91	0.24

Conditions: Solutions of TR of 0.01–0.7 mg/ml concentration range and *h*IgG with a concentration of 0.05–0.5 mg/ml were pumped at 2 ml/min flow-rate through CIM®-SBTI and *r*Prot G disks, respectively, at different temperature to produce the breakthrough curves; intermediate washing procedure was performed using 2 *M* NaCl and desorption step was carried out with 0.01 *M* HCl (pH 2.0); desorbed fraction of target protein was analyzed by Lowry test; K_{diss} and Q_{max} presented in the table are average values of those calculated from linearized forms of the Langmuire equation (Excel).

and *r*Prot G-*h*IgG. Similar experiments are rare in the field of affinity adsorption [34]. Table 6 summarizes our results and shows that $K_{diss.}$ values characterizing thermodynamic stability of affinity complexes do not depend strongly on temperature whereas the adsorption capacity (Q_{max}) for both studied pairs passes through a maximum at 15–20 °C. This suggests that the mechanism of strong affinity protein–protein pairing is more complex than that typical of weak pseudoaffinity interactions. In our case, the lower adsorption capacity at 40 °C cannot be explained by denaturation because of the absence of any irreversible changes of the affinity sorbent even after its long-term usage. Experiments targeted at this problem are currently in progress.

4. Conclusions

Very detailed investigations of the parameters of strong bioaffinity interactions carried out at different experimental conditions have been done. The data obtained have confirmed the possibility to produce very fast, flow and temperature independent affinity separations of a target substance from complex biological mixtures. Similar to the fictionalized membrane adsorbers, it has been shown that the fact of very small residence time of a separated solute inside suggested for these purposes that short layers of macroporous monoliths does not hinder from a biocomplementary pairing between immobilized and dissolved components. The different approaches of immobilization of biologically active ligands on GMA-EDMA materials and their influence of affinity binding parameters have been also studied and discussed in the paper.

5. Nomenclature

HPMDC	high-performance monolithic disk chromatography
HPMDAC	high-performance monolithic disk affinity chromatography
CIM®	convective interaction media
BSA	bovine serum albumin
TR	trypsin
CHTR	α-chymotrypsin
SBTI	soya bean trypsin inhibitor
OVA	ovalbumin
*r*Prot G	recombinant protein G
*h*IgG	human immunoglobulin G
PBS	phosphate buffered saline

Acknowledgements

We are grateful to Dr M.B. Tennikov for valuable discussions and methodological assistance. The project was partly founded by regional grant of SPb Department of RAS. BIA Separations d.o.o., Ljubljana, Slovenia is greatly acknowledged for providing CIM® disks.

References

[1] T.B. Tennikova, B.G. Belenkii, F. Svec, J. Liq. Chromatogr. 13 (1990) 63.
[2] T.B. Tennikova, M. Bleha, F. Svec, T.V. Almazova, B.G. Belenkii, J. Chromatogr. A 555 (1991) 90.
[3] F. Svec, T.B. Tennikova, J. Biocompat. Polym. 6 (1991) 393.
[4] T.B. Tennikova, B.G. Belenkii, F. Svec, M. Bleha, US Pat. 4,889,632 (1989); 4,923,610 (1990); 4,952,349 (1990).
[5] A. Štrancar, M. Barut, A. Podgornik, P. Koselj, Dj. Josic, A. Buchacher, LC-GC Int. 11 (1998) 660.
[6] T. Tennikova, R. Freitag, in: H.Y. Aboul-Enein (Ed.), Analytical and Preparative Separation Methods of Macromolecules, Marcel Dekker, New York, 1999, p. 255.
[7] T.B. Tennikova, R. Freitag, J. High Resolut. Chromatogr. 23 (2000) 27.
[8] C. Kasper, L. Meringova, R. Freitag, T. Tennikova, J. Chromatogr. 798 (1998) 65.
[9] J. Hagedorn, C. Kasper, R. Freitag, T. Tennikova, J. Biotechnol. 69 (1999) 1.
[10] G.A. Platonova, G.A. Pankova, I.Ye. Il'ina, G.P. Vlasov, T.B. Tennikova, J. Chromatogr. 852 (1999) 129.
[11] L. Berruex, R. Freitag, T.B. Tennikova, J. Pharm. Biomed. Anal. 24 (2000) 95.
[12] N.D. Ostryanina, G.P. Vlasov, T.B. Tennikova, J. Chromatogr. (2001) in press.
[13] Y.D. Clonis, Bio/Technology 5 (1987) 1290.
[14] S. Ohlson, L. Hansson, M. Glad, K. Mosbach, P.-O. Larsson, Trends Biotechnol. 7 (1989) 179.
[15] N.B. Afeyan, N.F. Gordon, I. Mazsaroff, L. Varady, Y.B. Yang, S.P. Fulton, F.E. Regnier, J. Chromatogr. 519 (1990) 1.
[16] N.B. Afeyan, S.P. Fulton, F.E. Regnier, J. Chromatogr. A 544 (1991) 267.
[17] M. McCoy, K. Kalghatgi, F.E. Regnier, N.B. Afeyan, J. Chromatogr. 753 (1992) 21.
[18] G.A. Heeter, A.I. Liapis, J. Chromatogr. 743 (1996) 3.
[19] G.A. Heeter, A.I. Liapis, J. Chromatogr. 761 (1997) 35.
[20] T.B. Tennikova, F. Svec, J. Chromatogr. A 646 (1993) 279.
[21] R. Hahn, A. Jungbauer, Anal. Chem. 72 (2000) 4853.
[22] I. Mihelic, T. Koloini, A. Podgornik, A. Štrancar, J. High Resolut. Chromatogr. 23 (2000) 39.
[23] M. Nachman, A.R.M. Azad, P. Bailon, J. Chromatogr. A 597 (1992) 155.
[24] P. Langlotz, K.H. Kroner, J. Chromatogr. 591A (1992) 107.
[25] F.T. Sarfert, M.R. Etzel, J. Chromatogr. 764 (1997) 3.
[26] K.-G. Brief, M.-R. Kula, Chem. Eng. Sci. 47 (1992) 141.
[27] E. Klein, J. Membr. Sci. 179 (2000) 1.
[28] J.A. Gerstner, R. Hamilton, S.M. Cramer, J. Chromatogr. A 596 (1992) 173.
[29] M.B. Tennikov, N.V. Gazdina, T.B. Tennikova, F. Svec, J. Chromatogr. 798 (1998) 55.
[30] O.H. Lowry, N.I. Posebrough, A.L. Farr, P.I. Randall, J. Biol. Chem. 193 (1951) 265.
[31] T.V. Gupalova, O.V. Lojkina, V.G. Palagnuk, A.A. Totolian, T.B. Tennikova, J. Chromatogr. (2001) in press.
[32] A.E. Rodrigues, J.C. Lopes, Z.P. Lu, J.M. Loureiro, M.M. Dias, J. Chromotogr. A 590 (1992) 93.
[33] A. Podgornik, M. Barut, A. Štrancar, Dj. Josic, T. Koloini, Anal. Chem. 72 (2000) 5693.
[34] G.M.S. Finette, Q.-M. Mao, M.T.W. Hearn, J. Chromatogr. 763 (1997) 71.